DTIC FILE COPY

NAVAL POSTGRADUATE SCHOOL
Monterey, California

DTIC
ELECTE
APR 9 1987

A

THESIS

LASER REFLECTANCE AS A FUNCTION OF
ROUGH WATER GLITTER PROFILE

by

Carlton M. Bourne

March 1987

Thesis Advisor   E. C. Crittenden, Jr.

Approved for public release; distribution is unlimited.

87   4 7 105

AD-A178 774

REPORT DOCUMENTATION PAGE

1a. REPORT SECURITY CLASSIFICATION UNCLASSIFIED		1b. RESTRICTIVE MARKINGS		
2a. SECURITY CLASSIFICATION AUTHORITY		3. DISTRIBUTION/AVAILABILITY OF REPORT Approved for public release; distribution is unlimited.		
2b. DECLASSIFICATION/DOWNGRADING SCHEDULE				
4. PERFORMING ORGANIZATION REPORT NUMBER(S)		5. MONITORING ORGANIZATION REPORT NUMBER(S)		
6a. NAME OF PERFORMING ORGANIZATION Naval Postgraduate School	6b. OFFICE SYMBOL (If applicable) 61	7a. NAME OF MONITORING ORGANIZATION Naval Postgraduate School		
6c. ADDRESS (City, State, and ZIP Code) Monterey, California 93943-5000		7b. ADDRESS (City, State, and ZIP Code) Monterey, California 93943-5000		
8a. NAME OF FUNDING/SPONSORING ORGANIZATION	8b. OFFICE SYMBOL (If applicable)	9. PROCUREMENT INSTRUMENT IDENTIFICATION NUMBER		
8c. ADDRESS (City, State, and ZIP Code)		10. SOURCE OF FUNDING NUMBERS		

		PROGRAM ELEMENT NO	PROJECT NO	TASK NO	WORK UNIT ACCESSION NO

11. TITLE (Include Security Classification)

LASER REFLECTANCE AS A FUNCTION OF ROUGH WATER GLITTER PROFILE

12. PERSONAL AUTHOR(S)
Bourne, Carlton M.

13a. TYPE OF REPORT Master's Thesis	13b. TIME COVERED FROM _____ TO _____	14. DATE OF REPORT (Year, Month, Day) 1987 March	15. PAGE COUNT 67

16. SUPPLEMENTARY NOTATION
This work was supported, in part, by the Naval Sea Systems Command
(NAVSEA 06W-30)

17.	COSATI CODES		18. SUBJECT TERMS (Continue on reverse if necessary and identify by block number)
FIELD	GROUP	SUB-GROUP	Laser radar altimeter, Reflectance of Sea Surface, Optical roughness of sea surface

19. ABSTRACT (Continue on reverse if necessary and identify by block number)

A new remote sensing technique was developed for predicting the expected mean laser radar return from a rough water surface. This technique involved measuring the standard deviations of the upwind and crosswind profiles of the elliptical glitter patterns occurring for illumination of the water surface with a point source near the laser radar system. A pencil beam laser radar from a companion project simultaneously measured the reflected signals from the water surface. The glitter pattern images were recorded with a video camera and recorder. The images for each run were later digitized along their major and minor elliptic axes and averaged over 256 images to produce smooth intensity curves from which the standard deviations were measured. The radar return fluctuated over a large range because of the rapid

20. DISTRIBUTION/AVAILABILITY OF ABSTRACT ☒ UNCLASSIFIED/UNLIMITED ☐ SAME AS RPT ☐ DTIC USERS	21. ABSTRACT SECURITY CLASSIFICATION UNCLASSIFIED	
22a. NAME OF RESPONSIBLE INDIVIDUAL E. C. Crittenden, Jr.	22b. TELEPHONE (Include Area Code) (408) 646-2855	22c. OFFICE SYMBOL 61Ct

DD FORM 1473, 84 MAR
83 APR edition may be used until exhausted
All other editions are obsolete

Block 19 contd.

variation of individual water surface facets, and so was recorded and time-averaged over the same interval as the video images. Data sufficient for empirical prediction of expected mean laser return signal were obtained. This is necessary to permit evaluation of the performance of a given laser radar design. The data obtained also approximated the predictions of a new model proposed in this work. *Keywords — , , field*

QUALITY
INSPECTED
1

Laser Reflectance as a Function of Rough
Water Glitter Profile

by

Carlton M. Bourne
Lieutenant Commander, United States Navy
B.S., United States Naval Academy, 1975

Submitted in partial fulfillment of the
requirements for the degree of
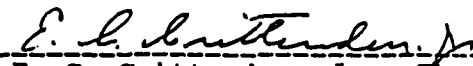

MASTER OF SCIENCE IN PHYSICS
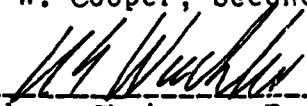

from the

NAVAL POSTGRADUATE SCHOOL
March 1987

Author: _____
Carlton M. Bourne

Approvedby: _____
E. C. Crittenden, Jr., Thesis Advisor

_____
A. W. Cooper, Second Reader

_____
K. E. Wohler, Chairman, Dept. of Physics

_____
G. E. Schacher,
Dean of Science and Engineering

3

ABSTRACT

A new remote sensing technique was developed for predicting the expected mean laser radar return from a rough water surface. This technique involved measuring the standard deviations of the upwind and crosswind profiles of the elliptical glitter patterns occurring for illumination of the water surface with a point source near the laser radar system. A pencil beam laser radar from a companion project simultaneously measured the reflected signals from the water surface. The glitter pattern images were recorded with a video camera and recorder. The images for each run were later digitized along their major and minor elliptic axes and averaged over 256 images to produce smooth intensity curves from which the standard deviations were measured. The radar return fluctuated over a large range because of the rapid variation of individual water surface facets, and so was recorded and time-averaged over the same interval as the video images. Data sufficient for empirical prediction of expected mean laser return signal were obtained. This is necessary to permit evaluation of the performance of a given laser radar design. The data obtained also approximated the predictions of a new model proposed in this work.

4

TABLE OF CONTENTS

ACKNOWLEDGMENTS

I. INTRODUCTION

A. BACKGROUND

The situation at the outset of this project was that a working model of an inexpensive, light, and compact laser radar altimeter, for use over the ocean surface, had been developed in this laboratory in a companion project [Ref. 1]. However, it had not been possible to relate its performance in the laboratory to real field performance with much certainty. The device determined the height above the water by measuring the time delay between the emission of a short laser pulse and the arrival of a return echo from the water surface. The limitations of size, weight, electrical power, and cost dictated a low power diode laser system. Additionally, there was a requirement of a finite divergence angle of the laser beam and associated detector optics in order to assure triggering of the time-delay measuring system in the event of a glassy calm and some angular wobble in the attitude of the laser system. These collective requirements meant that the primary design problem was that of achieving sufficient return signal from the water to assure triggering of the time delay circuits.

Evaluating the performance of the existing working model of a laser radar altimeter system over the water had the problem that the reflectance of a water surface is dependent on the roughness state of the water. The only data in the literature known to this author, which would permit an

estimate of the laser reflectance of rough water, are those of Petri [Ref. 2]. These data are rather meager, consisting of 16 separate measurements, and requiring a knowledge of the wind speed. The latter had been measured at a height of 60 feet above the water. The wind speed at the water surface was thus quite uncertain. Other data by Cox and Munk [Ref. 3] related the glitter pattern profile, for reflection of the sun, to wind speed over the ocean. Their optical data were taken from an aircraft at 2000 feet altitude, with windspeed measured on a ship at two heights, 9 feet and 41 feet above the water. It was not clear which of these two heights was used for quoting the wind speed. Their data also were not directed at evaluating the magnitude of the reflectance.

B. GENERAL OBJECTIVE

Preliminary field experiments, carried out as part of the work reported here, indicated that the reflectance of rough water could vary rapidly under changing wind conditions, and that knowledge of the wind speed at a given instant did not serve as a good indicator of the optical properties of the water surface at that instant. Additionally, if wind speed were to be measured, it probably should be measured very close to the water surface. This would be difficult, expensive, and in many cases impractical. The field work reported here for this project was carried out from high bridges, but it was intended that the

work would be extended later to aircraft. In that case the necessity for associated ship measurements of wind speed would be difficult logistically. Consequently, the objective of this work became to develop and demonstrate the feasibility of a remote sensing technique for evaluating the reflectance of a rough water surface at the instant of a laser radar altimeter test.

The papers of Cox and Munk, and Petri, taken together, led to a conclusion that it might be possible to predict an expected laser radar return on the basis of a measurement of the width of glitter patterns. It also seemed likely that glitter patterns measured with a nearly point source of light at night would be simpler to obtain and would yield more directly the desired result than would glitter patterns obtained with the necessarily oblique illumination from the sun. Consequently, the primary objective became to test the feasibility of prediction of laser return from the profile widths of glitter patterns obtained with a point light source. The early tests indicated that laser return was in fact a function of glitter pattern width. A tentative theoretical model was developed, which, although it has not as yet succeeded in predicting the observed absolute magnitude of laser return, does lead to a functional relationship which is useful. With the present semiempirical relationship, laser return can be related quantitatively to Lambertian return. Although more experimental data is needed to refine the results, and further

theoretical work is needed to clear up the discrepancy in the absolute values predicted by the model, laser return signals measured in the laboratory with Lambertian targets can now be directly related to field-expected values.

C. ASSOCIATED PROBLEMS

1. Laser Signal Fluctuation

There were several additional problems in carrying out the field experiments at the outset of this project. The laser radar altimeter model to be tested used a fairly narrow laser beam of 1.2 by 2.4 degrees divergence, with a 3 degree circular cone of acceptance of the receiver optics. This divergence had been chosen in the design process of the companion project as an optimization of the transmitter-receiver optics under the confines of required return signal magnitude and availability of inexpensive commercial components. This narrow beam was incident on the center of the "glitter" pattern, about which much more will be said later. The beam will be treated here as a pencil beam, essentially evaluating the peak value of laser return at the center of the glitter pattern. A consequence of the narrow beam geometry was that reflection of the laser beam from the water surface occurred at a relatively small and finite number of glint facets. As a result, the laser return signal fluctuated rapidly with time over a wide range of magnitude. This required recording the signal for later data processing to obtain the mean and

11

standard deviation of the variation. In order to accomplish the recording it was also necessary to provide a pulse stretcher because the laser return pulses were otherwise too short to handle with most analog FM data recorders.

Although the rapidly fluctuating magnitude of the laser return posed a measurement problem, it is helpful in the practical application of a laser radar altimeter. Measurement of range is accomplished by determining the time delay between the primary pulse and the return pulse. With fairly rapid pulse repetition rate, an occasional high pulse will serve to make the range determination practical, where the mean signal may not be above threshold for satisfactory operation. This feature tends to favor a small divergence beam. The statistics of this were not analyzed here but are left for later work. The data tape recordings from the field experiments are now available for such analysis.

2. Calibration by Means of Specular Reflection

Prior to the work reported here, optimization of design and laboratory evaluation of the laser radar altimeter had been carried out primarily using specular reflection from the outside of a plate glass window to obtain a return signal, after careful measurement of the inevitable slight surface curvature of the window. This permitted development of the time-difference circuitry and avoided the difficult problem of obtaining a water surface at sufficient range to be meaningful. The constant magnitude

of the return signals in this situation was also helpful in the development work. In evaluating the magnitude of the signal, the difference of reflectance of the two glass-air interfaces from that of a single water surface was easily accounted for. A rough evaluation of system performance was obtained in this manner, but the return signal, if maximized by angular adjustment to obtain the maximum signal, evaluated only the peak value of the central maximum of the laser beam, as will be discussed in Appendix B. To obtain a measure of the expected return signal from a rough water surface or a diffuse reflecting surface from the specular reflection data required carrying out a two-dimensional integration of the laser beam flux over the laser beam cross-section profile. The beam tended to have considerable detailed "banding" structure in its profile, making such evaluation rather doubtful.

3.   Calibration by Means of Lambertian Reflection

The problems attendant on use of specular reflection from a plate glass window to obtain a return signal are alleviated by use of a diffuse, "Lambertian" reflector such as a white sheet of paper. For a finite area, such a surface reflects a power proportional to the cosine of the angle of incidence. Such surfaces were used in the laboratory. However, the Lambertian surface must be large enough to include the entire transmitted laser spot. Hence at ranges sufficient to simulate real field conditions, the area required was large enough to make obtaining a good

13

uniform reflectance white surface difficult. The signals
with such a target would be constant in magnitude, except
for a small amount of atmospheric scintillation. At close
range, the signals were so large as to make circuit devel-
opment for small signal conditions difficult. Calibration
of the return signal magnitude can be done with a Lamber-
tian surface at close range, by careful attention to quan-
titative attenuation of the large return signal that would
otherwise saturate the receiver circuits. This sort of
calibration was done in the field tests to be reported
here. Finally there seemed to be no fully satisfactory way
to simulate all the circumstances to be encountered by a
real life laser radar altimeter, other than by field tests
over wind-roughened water. These were then initiated and
the accompanying remote sensing techniques reported here
carried out.

D. GENERAL METHOD

This work reports a new remote sensing system for esti-
mating the expected laser radar return signal through an-
alysis of glitter patterns. This is a remote sensing
method permitting determination of the expected reflectance
of a rough water surface using equipment colocated with the
laser radar altimeter. The equipment for this technique
also offers the advantage of being inexpensive and phy-
sically small for field use.

The time-averaged statistical distribution of light intensity was measured for images of glitter patterns produced by reflection of light projected onto the water from a small area incandescent source located near the laser altimeter. The images of the glitter patterns were recorded with a video camera, which avoided the nonlinearities of photographic recording and permitted digitization without intermediate steps. The magnitude of the returned laser signal was recorded at the same time that the video images were obtained. Because this signal was rapidly varying, it was recorded for statistical processing later. The resulting data related the mean laser return to the glitter pattern profile parameters. The results are most succintly expressed as a ratio of reflectance of the rough water to the reflectance of a (virtual) Lambertian reflector which reflects the same fraction of the total light as a water surface (0.0204) at normal incidence. Through use of data in other references, the return was also related to an inferred wind velocity for comparison. An analytical model was developed which seems to predict the correct functional behavior, although the predicted absolute magnitude of reflectance is at present out of line. Although these experiments should be repeated for refinement and completion, these results allow evaluation of a practical laser radar system by reflection from a Lambertian reflector within the laboratory, providing a more immediate and readily controlled environment for equipment development.

II THEORETICAL CONSIDERATIONS

A. GENERAL

When light from a small diverging source is incident on a water surface roughened by wind driven waves, it is reflected from the water surface in a glitter pattern, as seen by an imager located near the source. The glitter pattern is approximately elliptical in shape, with the major axis of the ellipse in the upwind direction, and the minor axis in the crosswind direction [Ref. 4]. The pattern is produced by specular reflection at a large number of rapidly changing facets located at the points where the surface is perpendicular to the incident light. A representative glitter pattern is shown in Figure 1.

Laser reflectance from calm waters can be readily calculated analytically [Ref. 5]. This is the case of specular reflection whereby a mirror image of the source is created equidistant below the water surface. Reflected energy appears to originate from this source.

At the other extreme from specular reflection is diffuse reflection. In this case a surface scatters incident energy over all angles in a hemisphere, resulting in a distribution called Lambertian, in which the reflected energy varies as the cosine of the angle from the perpendicular.

Figure 1. Glitter pattern produced by wind speed
of approximately 12 miles per hour.

Between these two extremes, an optically rough water surface exhibits properties of both types of reflection. The reflected intensity distribution varies according to the distribution of wave slopes scattering the incident beam. [Ref. 6].

B. GLITTER PATTERNS

The technique developed in this work was a method of evaluating the expected laser radar return from a water surface when it is roughened by wind. The technique is a remote sensing technique in that all measurements are made from the general location of the laser radar altimeter. Thus it does not involve knowing the windspeed at the water surface, nor any other meteorologic or oceanographic parameters. The measurements involve only the optical properties of the water surface. This is done by determining the size of the glitter pattern from a video camera recording of the reflection of an approximately point source of light near the laser radar. The laser radar used a pencil beam, so that it responded to the central maximum reflection point of the glitter pattern profile. The reflection from this fluctuated through a large range, as a function of time, so that a time-average of a recorded signal was required.

Cox and Munk have developed a method of measuring water surface roughness from photographs of sun glitter [Ref. 3]. The wave slope distribution was deduced from observations of sun glitter patterns, with the assumption that the wave slope distribution and the reflected light intensity distribution were the same. They found that a Gram-Charlier distribution was the best fit to the experimental data. This distribution function is

19

$$G = [1/(2\pi\sigma_u\sigma_c)] \times e^{-(X^2+Y^2)/2} \times$$

$$[1 - (1/2) C_{21}(X^2-1)Y - (1/6)C_{03}(Y^3-3Y) \quad \text{<-Skew}$$

$$+ (1/24)C_{40}(X^4-6X^2+3)$$

$$+ (1/24)C_{04}(Y^4-6Y^2+3) \qquad \text{Peak-edness}$$

$$+ (1/4) C_{22}(X^2-1)(Y^2-1) + ...]$$

(1)

or, $G = [1/(2\pi\sigma_u\sigma_c)] \times e^{-(X^2+Y^2)/2} \times [H]$

where $X = \Theta/\sigma_u$ with Θ the angle from vertical in the upwind/downwind direction, and

$Y = \mathrm{O}/\sigma_c$, with O the angle from the vertical in the crosswind direction.

The quantities σ_u and σ_c are the upwind and crosswind "standard deviations" for this distribution. For a Gaussian distribution the standard deviation is the root mean square deviation from the mean. The first two terms of the Gram-Charlier distribution are the same as for a Gaussian distribution. The Gram-Charlier sigma values are the values of sigma in the second term. As will be discussed later, the peakedness of the Gram-Charlier distribution causes these sigma values to be located lower on the curve than for a Gaussian distribution. The terms in the brackets in the Gram-Charlier distribution are a form of Hermite polynomial. These terms express the peakedness and skew of the function.

The Gram-Charlier distribution, above, is a two dimensional distribution. It is displayed as a function of

Θ and Φ in Figure 2. The dotted curves are the shape of a Gaussian with the same standard deviation values. The crosswind distribution is symmetric about the vertical but is more peaked than Gaussian. The upwind distribution is also more peaked than Gaussian, and has a skew in the upwind direction.

The Gram-Charlier distribution is a normalized function, i.e., with the complete Hermite polynomial series included, the integral of the function from minus infinity to plus infinity in X, and from minus infinity to plus infinity in Y, gives unity. At first sight it would seem that integration from minus infinity to plus infinity, over the angular variables used, is not strictly correct, as the angles can only go to $\pi/2$. The function as written above is an approximation, as it has only the first few terms of the Hermite polynomial included. However, Cox and Munk stated that this approximation was valid for all their data out to X = Y = 2.5. Contributions to the integral for values of X and Y beyond 2.5 are negligible, so that writing the integral as if it extended to infinity should be of no concern. The largest sigma values encountered in the data reported here were 7.5 degrees. For X = 2.5 this means the expression is taken to be valid to 19 degrees. The integrals written later in this thesis will express the limits as minus infinity to plus infinity, recognizing that the contributions of high X and Y are negligible.
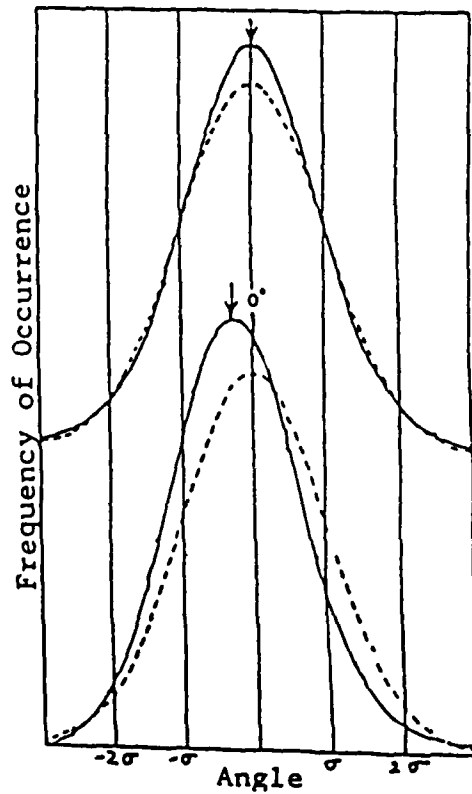
Figure 2. Wave slope distribution profiles deduced by Cox and Munk [Ref. 3]. Upper curves are taken along the Minor (Crosswind) axis of the elliptical pattern. Lower curves are taken along the major (up/downwind) axis. Solid curves are distributions deduced for a wind speed of 10 meters per second. Dashed curves refer to Gaussian distributions of the same standard deviation.

The extent to which the Gram-Charlier distribution exceeds the Gaussian due to the peakedness at the center can be evaluated by inserting the values of the coefficients, as given by Cox and Munk, and letting $X = 0$ and $Y = 0$. For the crosswind direction, the curve has no skew and the peakedness is independent of wind velocity. The coefficients for crosswind peakedness are

$$c_{40} = 0.40 \pm 0.23 ,$$

$$c_{04} = 0.23 \pm 0.41 , \tag{2}$$

and $\quad c_{22} = 0.12 \pm 0.06 .$

This gives a term multiplying the value of the peak as given by the first two terms of equation (1), i.e. the height of the Gaussian central peak is multiplied by a

factor $\quad f = 1.109 \pm 0.061 .$ $\qquad$ (3)

This factor will be used as 1.11 later.

For the upwind direction the skewness constants are

$$c_{21} = 0.01 - 0.0086W \pm 0.03 ,$$

and $\quad c_{03} = 0.04 - 0.033W \pm 0.12 , \tag{4}$

where W is the wind speed in meters per second. Although these constants depend on wind speed, they do not affect the area under the curve, and hence the normalization, as X and Y appear only in odd powers in the Gram-Charlier Hermitian terms. Thus whatever area they add for positive values of X or Y, they subtract for negative X or Y.

Although the skewness terms do not affect the peakedness for the crosswind direction, they do make a small contribution to the peakedness in the up/downwind

direction, but the contribution is small. For example, for
a wind speed of 10 meters per second, as illustrated in the
lower curve of Figure 2, the additional peakedness is
approximately two percent. The position of the peak is
also shifted slightly upwind. However, its position is
still within the "pencil" beam of 1.4 x 2.8 degrees used in
the laser radar altimeter here. The values for the predic-
ted laser return signal presented later in this thesis have
been adjusted for the skewness contribution to the peaked-
ness, even though this adjustment is in most cases the
order of one percent - really negligible in view of the 6
percent uncertainty quoted above from Cox and Munk on the
value of the peakedness factor.

To return to the meaning of the "standard deviations"
for the Gram-Charlier distribution, the standard deviation
values, σ_c and σ_u, are the standard deviations of the
Gaussian term of the Gram-Charlier form. In measuring
these quantities on an actual measured distribution, as
will be described later in this work, it is necessary to
measure the distribution curve width at a point lower by a
fraction 1.11 (or 1.12, depending on the skew contribution
to the peakedness for that particular curve) than the usual
0.659 times the peak value - the case for the usual Gauss-
ian distribution. This has been done in evaluating the
data later in this thesis.

A further fine tuning should also be noted. The peak-
edness terms in the Gram-Charlier distribution do produce

upward, or downward, displacements of the curve throughout the curve. This can be seen in the curves presented in Figure 2. Because of this displacement, it might seem that determination of sigma values by measuring the width of the peak at a height equal to 0.659/1.11 times the peak value, would be in error. (The factor 1.11 comes from equation (3) above.) To evaluate this effect, the coefficients in equation (2) above produce vertical displacements of the crosswind curve, i.e. for $Y = 0$, at $X = \pm 1$ (at the σ_c point), given by

$$1 + (1/24) \, c_{40} \, (1 - 6 + 3)$$
$$+ (1/24) \, c_{04} \, (3)$$
$$= 1 - .0333 \pm .0192$$
$$+ .0288 \pm .0513$$
$$= 1 - .0045 \pm .0547 .$$

This represents a downward shift of 0.4 percent, with an uncertainty of 5.5 percent. The 0.4 percent correction could be made by drawing a parallel line to the curve, shifted downward by that fraction, but it seems not worth doing in view of the 5.5 percent uncertainty. For the up/downwind curve the corrections are equally insignificant. Consequently such corrections have not been made during data reduction.

The most significant quantity, for this work, is the ratio of the peak of the distribution to the area under the distribution, as a function of the upwind and crosswind standard deviations. As mentioned before, the quantity, G,

25

in equation (1) above, is a statistical distribution. It is normalized so that the area under the curve is equal to unity, i.e.

$$\text{Area} = 1 = \int_{-\infty}^{\infty}\int_{-\infty}^{\infty} [1/(2\pi\sigma_u\sigma_c)]\ e^{-(X^2+Y^2)/2}\ [H]\ dX\ dY, \quad (5)$$

where the Hermitian peakedness and skewness terms have been abbreviated by the bracket [H].

The power per unit solid angle, I, reflected from a small spot on the water surface that is illuminated by the laser radar beam will have its reflected light spread into a cone where the intensity distribution varies according to the Gram-Charlier distribution. The magnitude of the solid angle of the cone will be taken to be that subtended by the glitter pattern, as observed at the detector. This assumption is discussed in Appendix D.

Letting I_o be the power per unit solid angle reflected perpendicular to the water surface and hence back to the detector of the laser radar, the power per unit solid angle in any direction will be given by

$$I = I_o\ \{2\pi\sigma_u\sigma_c/[H_o]\}\ G\ , \quad (6)$$

where $[H_o] = 1.11$ for peakedness at $X = 0$ and $Y = 0$.

As a verification of the statement in equation (6), note that at $X = 0$ and $Y = 0$,

$$G = G_o = \{1/(2\pi\sigma_u\sigma_c)\}\ [H_o]\ .$$

Hence at $X = 0$ and $Y = 0$,

$$I = I_o\ \{(2\pi\sigma_u\sigma_c)/[H_o]\}\ \{1/(2\pi\sigma_u\sigma_c)\}\ [H_o]\ ,$$

and $I = I_o$, as it should be.

Now the total reflected power is given by

$$P = \int_{-\infty}^{\infty}\int_{-\infty}^{\infty} I \, dX \, dY \ .$$

Inserting I from equation (6) gives

$$P = \int_{-\infty}^{\infty}\int_{-\infty}^{\infty} I_0 \ (2\pi\sigma_u\sigma_c/[H_0]) \ G \ dX \ dY \ .$$

Then from equation (5)

$$P = I_0 \ \{(2\pi\sigma_u\sigma_c/[H_0]\} \ . \qquad\qquad (7)$$

Now, the total reflected power, P, is the power radiated by the lasar radar in the pencil beam, P_0, multiplied by the Fresnel reflectance of water at normal incidence, r , or

$$P = rP_0 = rI_0 \ \{2\pi\sigma_u\sigma_c/[H_0]\} \ . \qquad\qquad (8)$$

Inverting gives

$$I_0 = rP_0 \ (1/2\pi\sigma_u\sigma_c) \ [H_0] \ . \qquad\qquad (9)$$

The flux at the detector, F_{og}, the power returned per unit area of the detector receiving optics, is given by I_0 times the solid angle subtended by a unit area at the detector optics, or

$$F_{og} = I_0 \ x \ 1/R^2$$
$$= rP_0 \ \{1/(2\pi\sigma_u\sigma_c)\} \ [H_0] \ /R^2 \ . \qquad\qquad (10)$$

C. FRESNEL REFLECTANCE

Use of the water reflectance for normal incidence in the preceding section perhaps needs some discussion. During the measurement of a glitter pattern the reflection at each glint is at normal incidence. Similarly, for the light scattered back to the laser detector from a pencil laser radar beam, the angle of incidence is again zero. On the other hand, for the light that does not return to the receiver because it is reflected out into an elliptic cone,

27

the angle of incidence at the reflecting facets is not zero. However, the contribution of scattered light for facets with angles of incidence greater than 2 sigma is negligible. Since the maximum sigma encountered in this work was 7.5 degrees, the variation of reflectance for angles of incidence of this magnitude needs to be examined.

The reflectance of a dielectric surface of index of refraction, n, as given by the Fresnel equations, for light with its electric vector perpendicular to the plane of incidence is

$$r_s = \left| \frac{\cos \Theta - (n^2 - \sin^2 \Theta)^{1/2}}{\cos \Theta + (n_2 - \sin^2 \Theta)^{1/2}} \right|^2 \tag{11}$$

For light with its electric vector parallel to the plane of incidence, the reflectance is

$$r_p = \left| \frac{-n^2\cos \Theta + (n^2 - \sin^2 \Theta)^{1/2}}{n^2\cos \Theta + (n_2 - \sin^2 \Theta)^{1/2}} \right|^2 . \tag{12}$$

At normal incidence, $\Theta = 0$ and $r_s = r_p = r$.

For unpolarized light at other angles, the total reflectance is $(r_s + r_p)/2$. The reflectance, r, at some representative angles, for water of index n = 1.333, at 16C, is

	Θ	r_s	r_p	r	Factor
Normal incidence	0°	.02037	.02037	.02037	1.000
	10°	.02133	.01944	.02038	1.001
	20°	.02449	.01662	.02055	1.009
	30°	.03093	.01194	.02144	1.053
	40°	.04316	.00585	.02450	1.203
	45°	.05299	.00281	.02790	1.370
Brewster's angle	53.1°	.07817	.00000	.07817	3.838
Grazing incidence	90°			1.0	

As can be seen from the above, the total reflectance for

unpolarized light varies very slowly with angle of incidence, even up to fairly large angles. The increase in reflectance is only 5% at 30 degrees. This is because r_p falls as r_s rises for angles less than the Brewster angle.

The results of Cox and Munk were also obtained using the same assumption as made here, i.e. that the reflectance of the water surface was constant and equal to the normal incidence value for all the angles encountered.

D. LAMBERTIAN REFLECTION

In order to compare calculations of predicted returned power to actual measured values, it is useful to relate glitter reflection to Lambertian reflection, where scattering is completely diffuse, as from a white sheet of paper. However the comparison will be made to a Lambertian type reflecting surface which reflects the same fraction of the total power on it as the reflectance for normal incidence from water, i.e. a fraction .0204 of the incident light is returned, when integrated over all angles within a hemisphere.

In general, for Lambertian reflection, the power per unit solid angle, I_{oL}, returned at perpendicular incidence, is given by

$$I_{oL} = P/\pi \tag{13}$$

where P is the total power reflected from the surface, integrated over all angles.

In the case of an idealized Lambertian water surface, the reflected power is given by

$$P = rP_o$$

where, as before, $r = .0204$ for the water surface.

The flux at the detector, the power returned per unit area, would then be given by

$$F_{oL} = rP_o/\pi R^2 . \tag{14}$$

This will be called the "Idealized Lambertian return flux". To summarize, it is the flux returning at normal incidence

from a Lambertian surface that reflects, integrated over all angles, a total fraction of the incident light equal to the reflectance of water for normal incidence (.0204).

E. EFFECTIVE REFLECTANCE

In order to characterize the optical state of the rough water surface, it is useful to define a quantity, ρ_{eff}, the effective reflectance of the water surface, as

$$\rho_{eff} = \frac{\text{Return flux from glitter}}{\text{Idealized Lambertian return flux}}$$

$$= \frac{F_{og}}{F_{oL}} \quad . \tag{15}$$

This quantity can be measured directly in terms of the ratio of laser radar return signals from a water surface to the signals from a Lambertian surface such as a white paper target, often at a different range from that of the water. This is discussed in detail later in this thesis, but to avoid confusion it should be mentioned here that the ranges of the water and the Lambertian target enter in that case, as well as the actual reflectance of the Lambertian surface used as a reference. In turn, the anticipated signal from a given model of a laser radar altimeter can be estimated, using a knowledge of the probable range of ρ_{eff} to be expected.

In terms of the model discussed in section A above, an idealized, or predicted, value of ρ_{eff} would be given by equation (15) after substituting expressions (10) and (14),

31

i.e.

$$\rho_{eff} = \frac{F_{og}}{F_{oL}}$$

or

$$\rho_{eff} = \frac{[H_o]}{2\sigma_u\sigma_c} \quad . \tag{16}$$

This will be called the idealized ρ_{eff}. The quantity $[H_o]$ is the magnitude of the Hermite polynomial for the two-dimensional Gram-Charlier distribution at normal incidence. $[H_o]$ had the numerical value of 1.11 in all cases encountered here. The quantity ρ_{eff} expresses the optical properties of a rough water surface, in terms of the standard deviations, σ_u and σ_c, of the glitter pattern. It is particularly useful because it does not depend on range and depends only on the optical state of the rough water surface.

The functional relationship expressed by equation (16) made it seem desirable to plot directly measured values of ρ_{eff} as a function of $1/(2\sigma_u\sigma_c)$. The results of such a plot are discussed later in this thesis. The measured values of ρ_{eff} did prove to vary linearly with $1/(2\sigma_u\sigma_c)$.

III. EXPERIMENTAL PROCEDURE

A. FIELD SITE

Experiments to measure laser reflectance as a function of glitter intensity profile were conducted from Parrott's Ferry Bridge over the New Melones reservoir near Columbia, California, following several earlier preliminary experiments at that site and at the Dumbarton bridge over San Francisco Bay. The Parrott's Ferry Bridge was the most favorable of many sites considered as it offered a fairly large distance to the water (109 feet at the time of the last experiments) and had a pedestrian walkway with no obstructions beneath. Heavy automobile traffic and inadequate pedestrian space, as well as obstructions beneath, made such sites as the Golden Gate Bridge and other bridges in the San Francisco Bay area unsuitable. It is hoped that funding for logistic support will be forthcoming so that these experiments can be continued from an aerial platform over open ocean.

The data reported here were all collected at the Parrott's Ferry Bridge on the night of 24 November, 1986, a clear night with no moon present. The wind speed varied from approximately 3 miles per hour to 12 miles per hour. Wind direction varied less than 30 degrees. Due to the short fetch in the reservoir, varying from 1/4 mile to 1 mile, depending on the direction, only high frequency waves and ripples were observed. It is anticipated that results

with these waves will scale up to ocean waves observed from higher altitudes.

B. LASER RADAR ALTIMETER SYSTEM

The laser system used was a working model of a laser radar altimeter, being developed by a companion project. The transmitter consisted of a 0.905 micrometer gallium arsenide diode laser driven by a pulser having a pulse width of 160 nanoseconds at half height. The transmitter output beam divergence was 1.4 degrees by 2.8 degrees. A silicon avalanche photodiode detector with an 8 mm focal length lens was used to receive the reflected laser signal. The aperture field of view was circular with a divergence angle of 3.6 degrees, totally encompassing the area illuminated by the transmitter. A 10 nanometer bandwidth multilayer film filter was included in the detector optics to eliminate noise due to sunlight, for daylight operation. The laser system was mounted on an arm extending 3 feet from the bridge railing. There were no bridge supports or obstructions near enough to produce unwanted reflections. The laser was 109 feet above the water.

The detector output was continuously displayed on a portable oscilloscope. Because the pulse length of the returned laser pulses was only 160 nanoseconds, it was necessary to stretch the received pulses electronically and assemble them to form a continuous-wave analog signal to permit recording. By the Nyquist theorem, the maximum

34

component frequency of this signal is limited to 500 Hertz by the interpulse interval of one millisecond. It was thus possible to record this signal on a frequency-modulated analog tape recorder, a Hewlett-Packard HP-3960A recorder, which had a signal bandwidth of dc to 20 kilohertz. The signals were recorded simultaneously with recording of the video pictures of the glitter pattern. Synchronization of the video recordings and laser return signal recordings was accomplished by recording the same voice track on both recorders.

The laser return signal magnitude was later data-processed in the laboratory with a DATA Precision Corp. DATA-6000 waveform analyzer to yield a mean laser return signal. As the laser return signals were played back from the recorder into the analyzer, 16 sequential waveforms, each consisting of 512 data points taken at 1 msec intervals, were averaged. This process was repeated 5 times for each run and these were averaged to obtain a mean value. Successive averagings of slightly different regions within the ten seconds over which the video signals were averaged yielded a standard deviation for the magnitude of the mean signal.

C. LASER REFERENCE MEASUREMENTS

An effective Lambertian water reflectance signal was obtained by means of measurements of the laser return signal from a white sheet of paper. These measurements

35

were made in the field shortly after the measurements of water reflectance signal. The white paper sheet was located at a distance of 39 feet. At this distance the transmitted laser pattern was still fully within the boundaries of the sheet of paper. The same paper was separately calibrated in the laboratory and found to reflect 0.73 times as much light at normal incidence as a perfect Lambertian surface. This value is representative of most white paper surfaces. The calibration procedure is discussed in Appendix B. The *effective* Lambertian water return signal was then obtained by multiplying the signal from the white sheet of paper at 39 feet by the ratios

$$(.0204/0.73) \times (39/109)^2 \, .$$

The factor (.0204/0.73) takes account of the difference in reflectance of the white paper sheet and the idealized Lambertian water surface. The factor $(39/109)^2$ takes account of the different distances of the white sheet and the water, 39 and 109 feet respectively. The inverse square law applies to these distances.

The *effective* reflectance coefficient, ρ_{eff}, as defined in section II E, was then calculated by dividing the mean laser water return signal by the *effective* Lambertian water return signal. i.e

$$\rho_{eff} = \frac{\text{Mean laser return signal}}{\text{Idealized Lambertian water return signal}} \, .$$

D. GLITTER PATTERN MEASUREMENT

Glitter patterns were produced by illuminating the water surface with a quartz-halogen lamp of a type used as a light source in overhead classroom projectors. This produced a nearly uniformly illuminated patch on the water with a total beam angular divergence of about 60 degrees, considerably wider than any of the observed glitter patterns. The uniformity of the illumination was verified in the laboratory in advance. The lamp was rated at 360 watts at 54 volts. Power for this lamp was provided by a small rotary converter generating nominal 120 volts, 60 Hertz power up to 500 watts, and driven by 12 volts dc from an automobile-type storage battery. The lamp voltage was varied, as needed, by means of a variac. The video camera was an RCA type TC2055C with a Vidicon tube. It was operated on 12 volts dc directly from a second automobile storage battery. The camera performance was very stable as it generated its own line-scan frequency with a quartz oscillator. The HP3960A FM data recorder for the laser radar signals also operated with 120 volt 60 Hertz power, obtained from this same battery through a frequency controlled square wave chopper converter. The video images from the RCA camera were recorded on a portable 8mm video tape recorder that was part of an Olympus VX-801-KU 8mm video camera system. This system also displayed a continuous monitor image of the scene as viewed by the RCA

37

camera. This allowed the brightness level of the illumination to be adjusted for proper recording and also permitted alignment of the camera with the major or minor axis of the elliptic glitter pattern. The 8 mm tape system was very compact and operated on its own internal batteries. As measured in the laboratory, the resolution of this combined system exceeded that of the usual home VHS format by about 20%.

The lamp and video camera were mounted on an arm extending from the bridge railing at a point about 6 feet from the laser altimeter. The video camera was oriented first along, then across, the wind direction, so that sequentially the major and then the minor axis of the elliptical glitter pattern would be aligned horizontally in the recorded video image. The 16 mm camera lens was focused at infinity with an aperture setting of f/1.6 . The 16 mm focal length gave a wide enough field of view to include the complete glitter pattern in every case. Recording sequences of 15 to 30 seconds were made at several different illumination levels in order to be sure to avoid saturating the camera.

Later, in the laboratory, the 8 mm video tape recordings were copied into a Sony Superbeta VCR which had more flexible reproducing features than the 8 mm field unit. The resolution of this VCR was previously measured and found to exceed that of the usual home VHS format by 50%. No detectable degradation occurred in this copying process.

The output of the video recorder was sent to a Tektronix 468 digital oscilloscope. Successive single horizontal TV scan lines, lying along, or perpendicular to, the glitter pattern major axis, were displayed on the scope using the "B sweep delayed" mode. The waveform displayed was a time-varying signal proportional to the intensity distribution along the major or minor glitter pattern elliptic axis. The oscilloscope was then set up to digitize and average 256 such sweeps and to store the accumulated waveform. The real time period represented by the 256 sweeps was 256/30 or 8.5 seconds. The computer program in appendix A was written to allow the Tektronix 468 to interface with an IBM PC/XT through an IEEE488 interface bus [Ref. 7]. With the computer as controller for the operation, the oscilloscope digitized and transmitted the waveform data to the computer. The digital information was then stored in memory or on disk for further processing.

The Tektronix oscilloscope was then adjusted so that it displayed a TV line through an image of the prevailing water surface outside the glitter pattern. Sweep averaging and transmission of a waveform to the computer memory were again carried out. This provided a background signal which was subtracted from the glitter waveform in the computer. The computer was then programmed to plot the glitter pattern profile on an Epson FX80 dot matrix printer. Figures 3 and 4 show the resultant intensity profiles along the

RELATIVE INTENSITY

1.0

0.5

0.0

9   6   3   0   3   6   9

POSITION IN GLITTER PATTERN

(Degrees off TV camera axis)
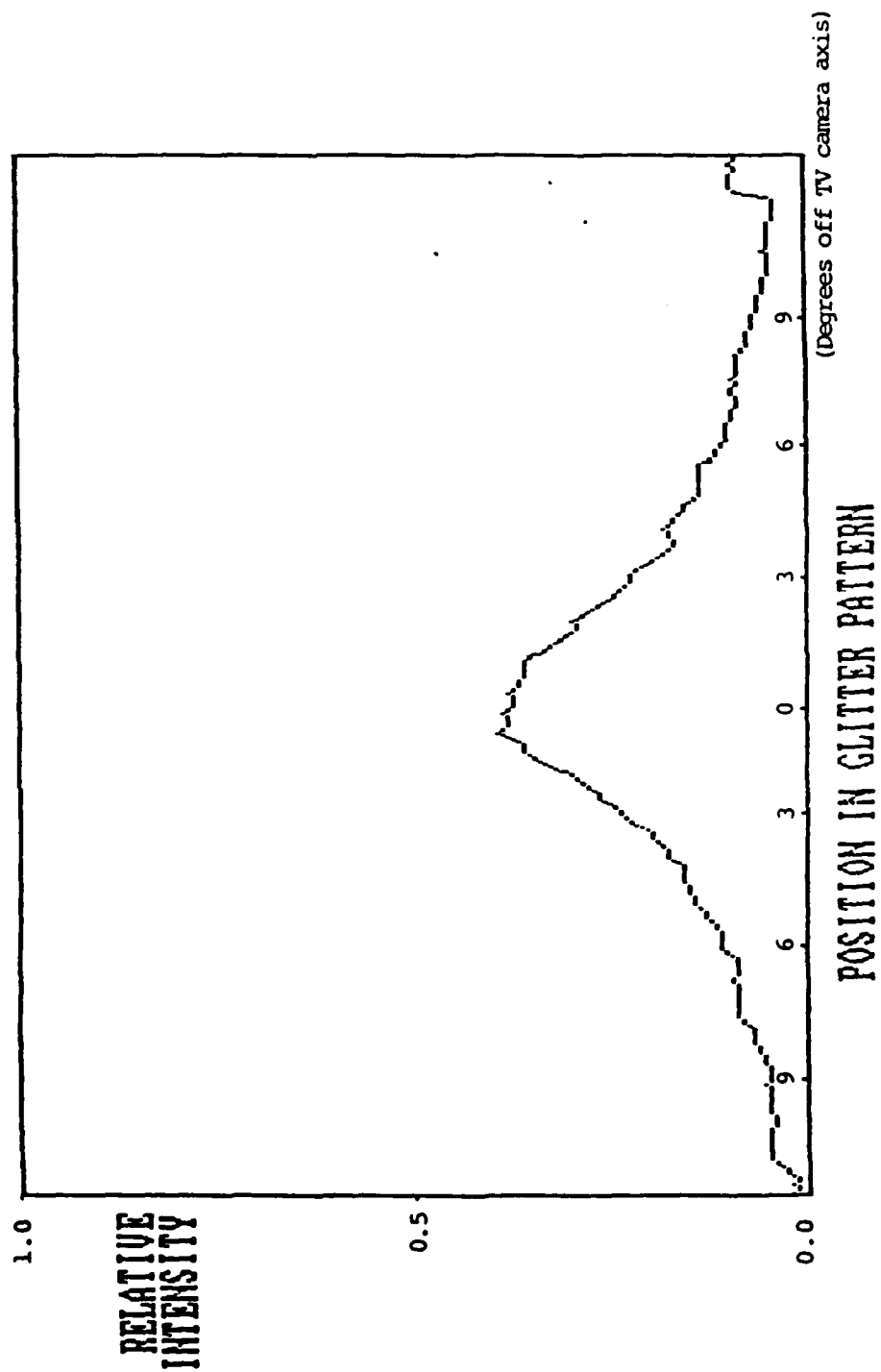
Figure 3. Upwind Glitter Pattern Intensity Profile

Figure 4. Crosswind Glitter Pattern Intensity Profile

POSITION IN GLITTER PATTERN

(Degrees off TV camera axis)

RELATIVE INTENSITY

41

major and minor elliptic axes from a representative run. Gram-Charlier standard deviation values σ_u and σ_c were then measured graphically from these profiles by measuring the half width at a height equal to 0.659/1.11 times the peak value, as discussed earlier.

IV. RESULTS

The measured values of ρ_{eff}, the ratio of observed laser radar return to that expected for Lambertian reflection, were plotted as a function of the corresponding values of $1/(2\sigma_u\sigma_c)$, in Figure 5, where σ_u and σ_c were the measured upwind and crosswind Gram-Charlier standard 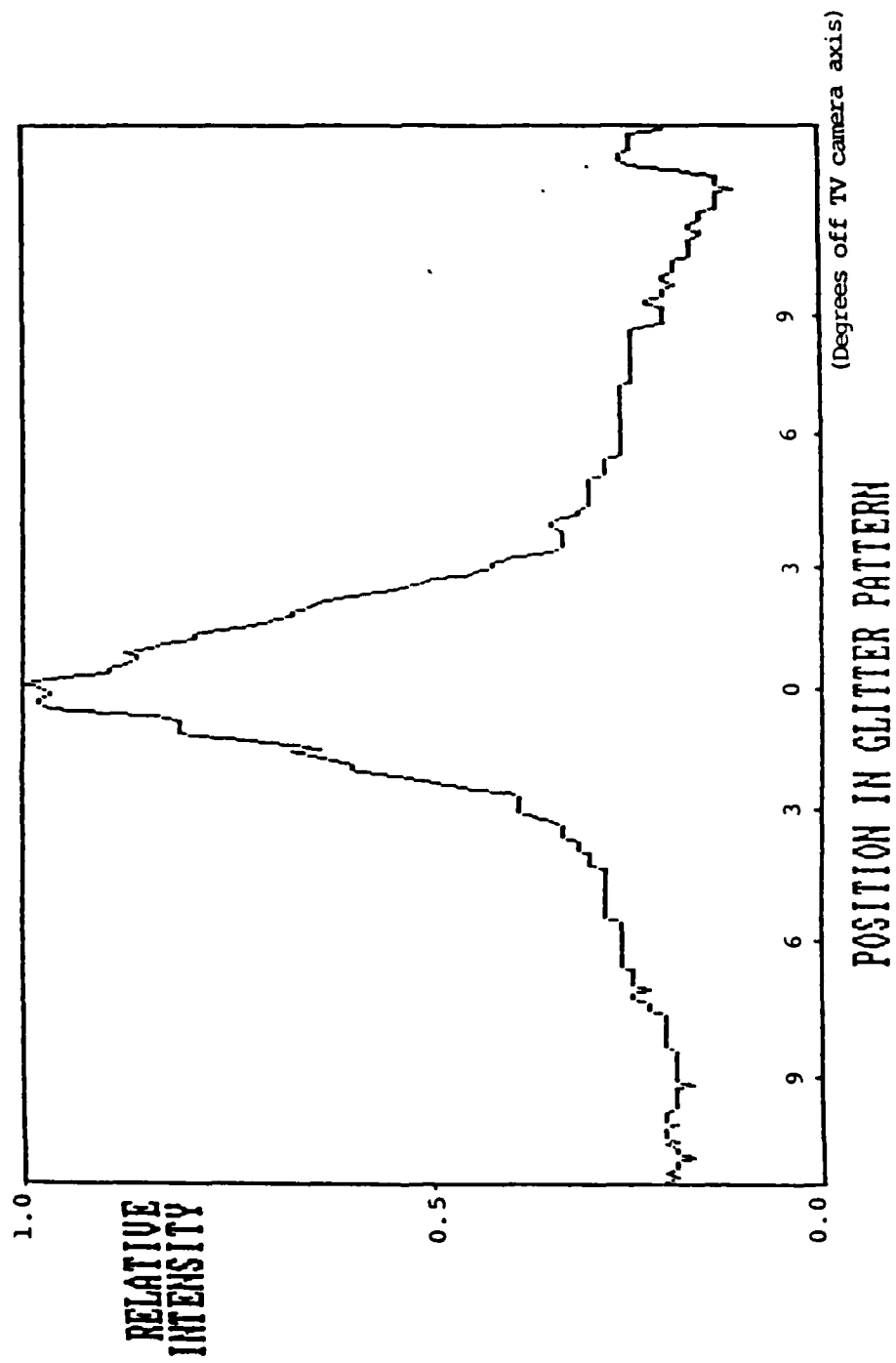deviation values for the glitter patterns. The data values are tabulated in Appendix C. Use of the function $1/(2\sigma_u\sigma_c)$ for the abscissa was suggested by the model discussed in section II. This functional form organized the experimental points so as to fall fairly well along a straight line. The solid straight line was a least squares solution for the data points taken here, shown as the circles in that figure. The correlation coefficient was $r = 0.96$ for the points relative to this line. This line had a slope of 0.92 and an intercept of 44 on the ordinate axis.

This empirical relationship provided a basis on which to predict the expected reflectance of a pencil beam from a rough water surface on the basis of only the remote sensing measurement of the glitter pattern profile. This made possible the field evaluation of working models of laser radar altimeters with the help of a simple technique. The functional relationship, and also the body of data were the first of this sort in this field. Without this technique, the field performance of a given laser altimeter system would require expensive concurrent logistic support to
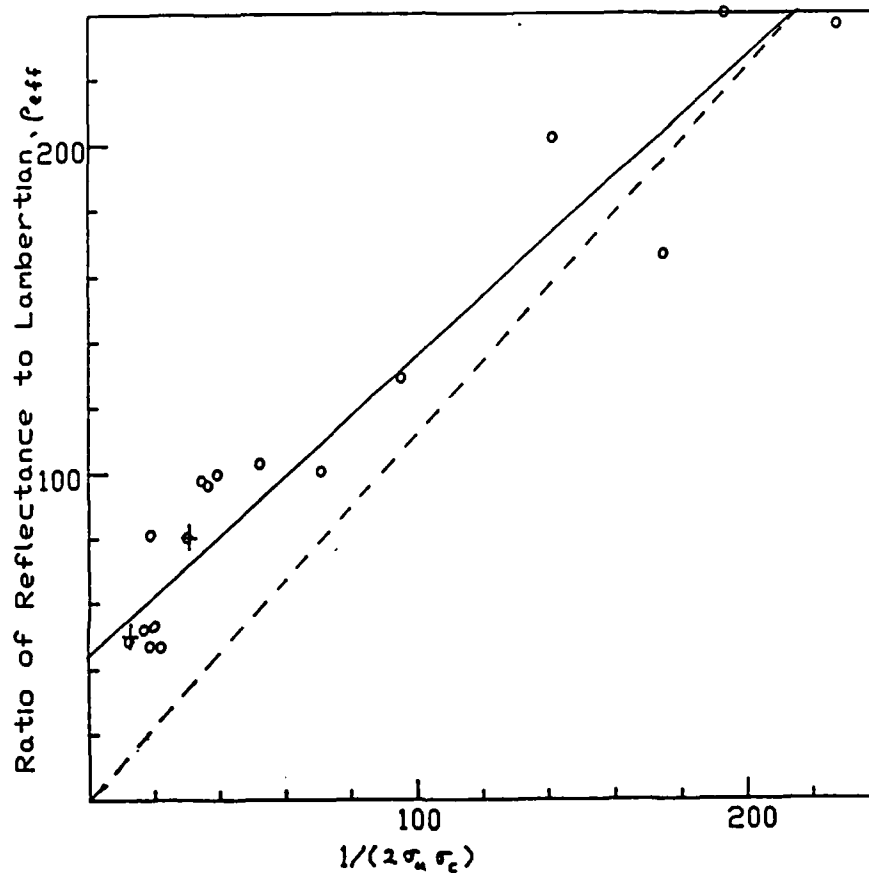
Figure 5. Observed effective reflectance relative to Lambertian, ρ_{eff}, as a function of $1/(2\sigma_u\sigma_c)$, plotted as circles. The solid line is a least squares fit of a straight line to these points. Two data points plotted as crosses are based on Petri's data [Ref. 2]. The dashed line represents an ideal model proposed in this thesis.

determine the roughness state of the water. The latter was likely to be inferred from meteorological and oceanographic data, and to be only the deduced probable steady state condition, whereas the technique reported here directly measured the momentary optical state of the ocean surface.

The numerical values of ρ_{eff} were of immediate utility. The lowest value, represented by the intercept on the y axis, was 44. Although extrapolation to the axis had considerable uncertainty, it did imply that for the worst case the ratio of reflectance to that for Lambertian was considerably above unity, at least by somewhat over one order of magnitude. Without evidence such as this, a working altimeter would presumably have had to be designed to cope with a case where a unity ratio to Lambertian might have occurred. This factor of 44, or somewhat over one order of magnitude increase in signal, represented a large reduction in the design requirement to be sure of a return signal. This had immediate importance in the ability to achieve the *design requirements.*

That the observed signals were directly relatable to reflection from a Lambertian surface made it possible to do most of the testing work in the laboratory. Various evolutions of laser radars could be tested with a Lambertian surface such as a white sheet of paper. The signals could then be scaled to those for a water surface at any required distance. The range of field signal return values could then be evaluated in terms of Figure 5.

The model proposed in Section IIB, which predicted that $\rho_{eff} = [H_o]/(2\sigma_u\sigma_c)$, required a straight line through the origin with slope $[H_o] = 1.11$ in Figure 5. This is represented by the dashed line in that Figure. An alternative prediction is for the slope to be $[H_o]/4$, depending on the view taken regarding the solid angle of the return scattering cone, as described in Appendix D. Although neither alternative represented a good fit, the data points did lie along a straight line, with slope not far from 1.11 . The existence of a theoretical model that agreed with the observed behavior in more detail would have been desirable, but it was not necessary. The present experiment had achieved the stated objective of providing a means of determining the optical state of the rough water by a remote sensing technique, where none existed before this work. The result was semiempirical, but was useful.

The fact that the proposed model did not predict the observed behavior could be viewed as an interesting challenge. That the observed effective reflectance was larger than expected, by somewhat less than a factor of four, and that the straight line had an intercept, indicated that this was a problem unlikely to be related to miscellaneous small increases or losses of light. Some of the immediate, ad hoc, explanations of this discrepancy that come to mind, seemed to predict less reflectance, rather than more. For example, if the variation of specular reflectance with angle were invoked for light reflected at large angle of

incidence into the far wings of the Gram-Charlier distribution, then less light should have returned along the axis, rather than more.

Another effect producing deviation toward too little reflection was that the laser "pencil" beam had a finite divergence of 1.4 by 2.8 degrees. Thus the reflectance was really the average over the curved top of the Gram-Charlier distribution. Thus the average observed would have been slightly less than the peak value. Correction for this is planned in subsequent work, but this correction will produce an increase in the peak reflectance, rather than a decrease, as needed to fit the model.

A possibility, in the right direction, in that it would have tended toward producing the higher than expected values of reflectance, was that some spray might have begun to develop as the wind increased. This would have corresponded to the region of small values of $1/(2\sigma_u\sigma_c)$. The droplets would have acted as retroreflectors and increased the returned signal along, or near, the laser beam axis. This effect, called the "glory", is commonly seen in looking down from an aircraft in the direction of the shadow of the aircraft. However, this explanation seemed quite unlikely in view of the low sea state encountered on the reservoir.

As to the major factor of four, it appeared that there was no real reason to omit it. The belief that it possibly lay in misinterpretation of the solid angle of the return cone of light had its only real motivation in that the

47

alternative choice led to a factor of four. It seemed more likely that the trouble was fundamental, perhaps lying in the assumptions made by Cox and Munk, and others, that the light was reflected by infinitesimal flat facets, rather than by a statistical average over focusing curved surfaces, where the surfaces fortuitously curved to be retroreflectors contributed disproportionally high return signal. Such an effect seemed likely to be much more pronounced with a nearly point source at short range, as used here, than for the case of the sun as an extended source at infinite range, as used by Cox and Munk. This point is expected to receive more attention in the succeeding work on this project.

V. COMPARISON WITH OTHER RESULTS

Direct comparison of the results reported here with those of others was possible only for one bit of fragmentary data. No other measurements of laser reflectance as a function of glitter pattern width were known to the author, except for a single diagram in the article by Petri [Ref. 2]. The values of glitter pattern width were not quoted there, as the article was primarily concerned with measuring the peak reflectance as a function of wind velocity. However, a few sample glitter pattern profiles were shown in one figure. That figure is reproduced here as Figure 6. It was possible to measure the sigma values graphically from these curves, although the curve shapes were poor. Those curves were obtained by a laser scanning in a vertical plane, with the plane rotating slowly through 360 degrees about a vertical axis. The scans were averaged so that no information was retained on the relative magnitude of upwind and crosswind sigma values. Two of these curves yielded sigma values that could be related to the results in this thesis. The others were too poorly resolved or they corresponded to reflectivity above or below the range measured in this work. Two pairs of these curves were for essentially the same windspeed so that an estimate of the internal consistency could be made. These pairs differed by 12% and 14% for the peak value. Points for the two utilizable widths were plotted with the symbol + on

49

27 Jun - 3 mph (estimated)

28 Jun - 7.4 mph

*29 Jun - 9.6 mph

4 Oct - 9.6 mph
*29 Jun - 10.4 mph

29 Jun - 10.8 mph

5 Oct - 13.7 mph

5 Oct - 16.9 mph

Relative Averaged Return Power

0.7
0.6
0.5
0.4
0.3
0.2
0.1

-24.00   -16.00   -8.00   0.0   +8.00   +16.00   +24.00
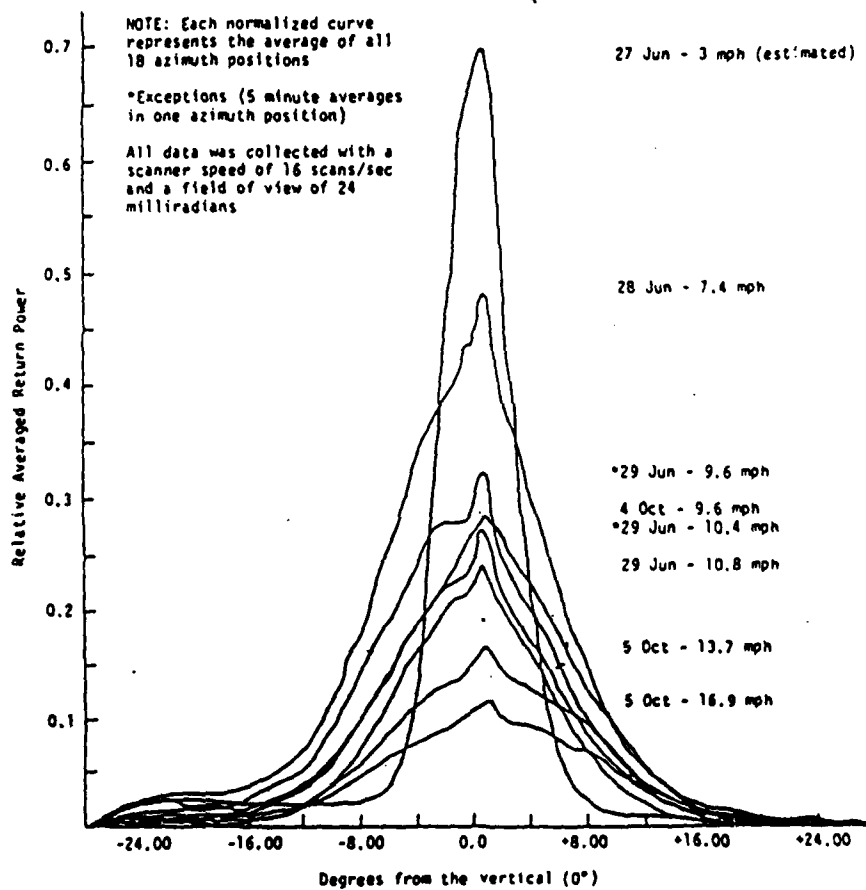
Degrees from the vertical (0°)

Figure 6. Normalized average return signal versus
laser/receiver angle as reported by Petri [Ref. 2].

50

Figure 5 of this thesis. They fell close to the data points obtained in this work.

Although the results obtained in the work reported here were intended to provide a means of evaluating laser radar altimeter performance without the necessity of knowing the wind speed, it was interesting to relate these results to data taken by others, where the wind speed was measured. This provided some confirmation of the validity of the results reported in this thesis.

An indirect comparison, where an inferred wind speed allowed intercomparison with related experimental data in the literature, was possible by combining the results of Petri [Ref. 2] with the results of Cox and Munk [Ref. 3]. Petri reported laser reflectance data in terms of wind speed for waves under the Chesapeake Bay bridge near Annapolis, Md. Figure 7 reproduces the results of Petri for laser return as a function of wind speed, with his results plotted as the crosses. No theoretical model was offered in that article.

Cox and Munk gave a relationship between their measured wind speed and the mean square upwind and crosswind sigma values for the glitter patterns, where W was the wind speed in meters per second, as

$$\sigma_c^2 + \sigma_u^2 = .003 + 5.12 \times 10^{-3} \, W \pm .004 \quad .$$

W has been called the effective wind speed here, as it was only a means to cross-connect to the data of Petri. Using the above expression, effective wind speeds were calculated
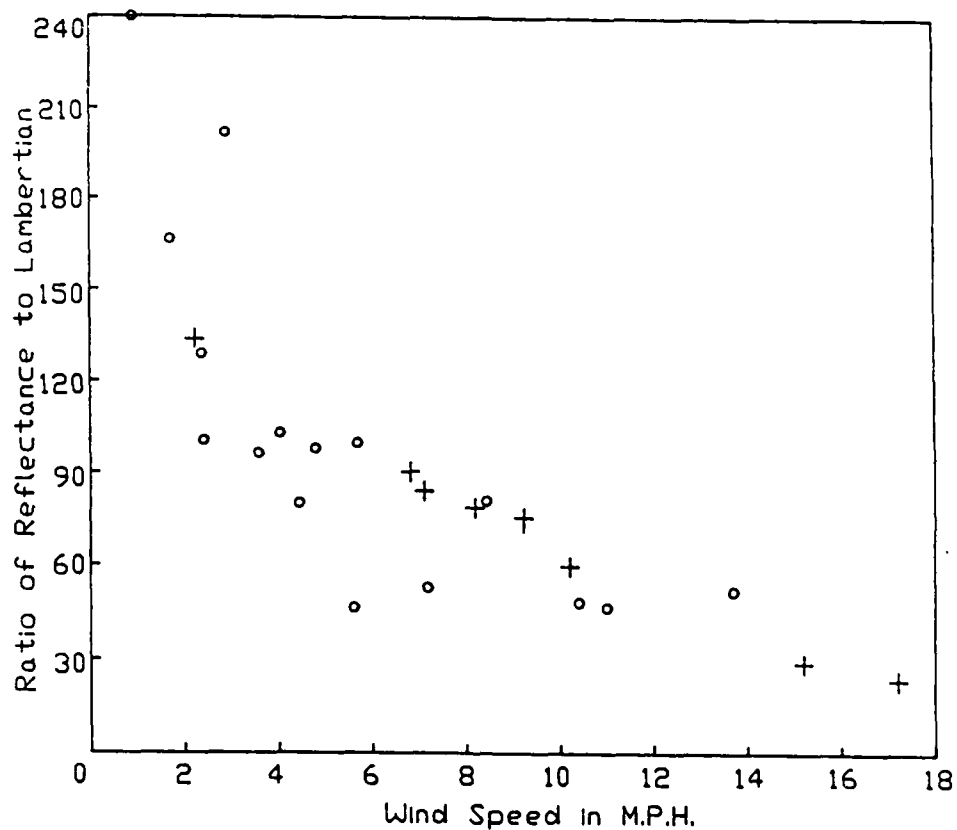
51

Figure 7. Plot of observed effective reflectance relative to Lambertian, ρ_{eff}, versus wind speed. Circles represent reflectance data obtained in this work plotted versus inferred wind speed. Crosses represent reflectance data collected by Petri plotted versus measured wind speed [Ref. 2].

for our data. The corresponding laser returns are plotted as the circles in Figure 7. It can be seen that the data points from both sources cluster into a broad band in the same general region.

The approximate agreement of the data reported here with the combined results of Petri and Cox and Munk gave some credence to the ability to relate laser radar return to the width of glitter patterns.

It should be pointed out again that the purpose of this work was to obtain a measure of expected laser radar return signal from rough water by remote sensing techniques and without a knowledge of wind speed. The effective wind speed deduced from the expression of Cox and Munk was useful only to permit the cross-connection to Petri's data. These wind speeds should be considered here only as a means of obtaining order of magnitude confirmation of the optical results. Intercomparison was somewhat doubtful because the Cox and Munk data were for open ocean waves, with wind speeds measured at 9 and 41 feet above the water. The Petri results were for waves under the Chesapeake Bay bridge near Annapolis, Md, with wind speed measured at 60 feet above the water. In spite of these uncertainties in wind velocity it was interesting that utilization of these results yielded approximate agreement between the data reported here and that of Petri.

VI. CONCLUSION

This work showed the feasibility of a remote sensing technique for determining the expected magnitude of laser radar return from a rough water surface by measurement of the size of a simultaneously measured elliptical glitter pattern. The technique did not require any additional knowledge of the water surface beyond optical measurements made at the location of the laser radar altimeter. No previous such technique had been in existence. The effective laser reflectance, ρ_{eff}, proved to vary approximately linearly with $1/(2\sigma_u\sigma_c)$, where σ_u and σ_c are the Gram-Charlier standard deviations for the upwind and crosswind glitter pattern intensity profiles, respectively. ρ_{eff} is the ratio of the laser radar return signal to the laser radar return signal to be expected from the water if it were to act as a Lambertian, diffuse reflecting, surface but with an overall reflectance coefficient equal to that for normal incidence for water. A least squares fit to a straight line gave a slope of 0.92 and a y intercept of 44, with a correlation factor, $r = 0.96$.

Plotting ρ_{eff} as a function of $1/(2\sigma_u\sigma_c)$ was suggested by the model proposed in this thesis. That model indicated that a straight line for ρ_{eff} as a function of $1/(2\sigma_u\sigma_c)$ should pass through the origin with a slope of $[H_o]/4$, or perhaps a slope of $[H_o]$, where $[H_o] = 1.11$, under a different, controversial, interpretation. The solution to the

54

discrepancy between the observed data and the suggested model is a problem that remains for further work.

That the straight line did not go through the origin, but instead had an intercept of 44, provided important information. This said that the worst case of very rough water should provide a return signal 44 times the magnitude of that from a water Lambertian surface. Although such extrapolation completely to zero is risky, it implied that for very rough water the smallest laser radar return is somewhat more than one order of magnitude larger than would have had to be assumed in the absence of this information. This would permit the design of a laser radar altimeter with an order of magnitude less power than would have to be assumed otherwise.

Finally, the existence of these results provides a firm relationship between the reflectance of a rough sea surface and that of a Lambertian surface, such as a large white surface at limited range in the laboratory. This reduces the need for field tests of various working models of laser radar altimeters.

APPENDIX A

COMPUTER PROGRAM

```
10 DIM Y(520),DTA(520),BACGND(520
20 DEF SEG = &HD000
25 KEY OFF
30 INIT = 0                        'ASSIGN OFFSET ADDRESS OF INIT
40 ADDR% = 21                      'CONTROLLER ADDRESS
50 LEVEL% = 0
60 CALL INIT(ADDR%, lEVEL%)
70 TRANSMIT= 3 :RECEIVE = 6        'OFFSET ADDRESSES
80 CMD$      ="MLA TALK 3"         'MY LISTEN ADDRESS
90                                 'DEVICES' TALK ADDRESS
100 CALL   TRANSMIT  (CMD$,STATUS%)
110 PRINT   "TRANSMIT STATUS = ",STATUS%
120 R$ = SPACE$(255)               'SET LENGTH OF R$>= LENGTH
130 R1$ = SPACE$(255): R2$ = SPACE$(255)
140 PRINT "Set up for data - push any key when ready "
150 V$=INKEY$:iF V$="" THEN 150
160 CLS                            'OF THE INCOMING DATA
170 CALL RECEIVE(R$, LENGTH%,STATUS%)
180 PRINT "RECEIVE STATUS = ",STATUS%
190 CALL RECEIVE (R1$,LENGTH2%,STAT2%)
200 PRINT "RECEIVE STAT2 = ",STAT2%
210 CALL RECEIVE(R2$,LENGTH3%,STAT3%)
220 PRINT "RECEIVE STAT3 ",STAT3%
230 IF STATUS%<>0 THEN PRINT"RECEIVE ERROR TRY AGAIN";GOTO
    100
240 FOR I = 178 TO 255
250 DTA(I-177)=ASC(MID$(r$,i))
260 NEXT I'270 PRINT R$,R1$,R2$
280 FOR I=1 TO 255
290 DTA(I+78) = ASC(MID$(R1$,i00
300 NEXT I
310 FOR I= 1 TO 180
320 DTA(333)=ASC(MID$(R2$,I))
330 NEXT I
340 FOR I=1 TO 520 STEP 10
350 FOR J = 1 TO 10
360 PRINT USING "     ###";DTA(I+J-1);
370 REM LPRINT USING"     ###";dta(I+J-L);'380 NEXT J
390 PRINT
400 REM LIST
410 NEXT I
420 INPUT "DO YOU WANT THE DATA RECORDED? Y/N", ANS$
430 IF ANS$ = "n" OR ANS$ = "N", THEN GOTO 580
440 INPUT "INPUT FILE NAME", FILEN$
450 IPUT "input header",A$
460 OPEN FILEN$ FOR OUTPUT AS #1
```

```
470 PRINT #1,A$
480 PRINT #1, MID$(R$,1,80)
490 PRINT #1, MID$(R$,81,80)
500 PRINT #1, MID$(R$,161,13)
510 PRINT #1, DATE$, TIME$
520 FOR I=1 TO 520 STEP 10
530 FOR J=1 TO 10
540 PRINT #1, USING "     ###";DTA(I+J-1);
550 NEXT J
560 PRINT #1," "
570 NEXT I
580 R$ = SPACE$(255)                    'SET LENGTH OF R$>=LENGTH
590 R1$ = SPACE$(255): R2$ = SPACE$(255)
600                                     'OF THE INCOMING DATA
610 PRINT "Set up for background - push any key when ready "
620 V$=INKEY$:IF V$="" THEN 620
630 CLS
640 CALL TRANSMIT(CMD$,STATUS%)
650 PRINT "TRANSMIT STATUS = ",STATUS%
660 CALL RECEIVE(R$, LENGTH%, STATUS%)
670 PRINT "RECEIVE STATUS = ", STATUS%
680 CALL RECEIVE(R1$,LENGTH2%,STAT2%)
690 PRINT "RECEIVE STAT2 = ",STAT2%
700 CALL RECEIVE(R2$,LENGTH3%,STAT3%)
710 PRINT "RECEIVE STAT3 = ",STAT3%
720 IF STATUS%<>0 THEN PRINT"ERROR READING DATA ":GOTO 580
722 IF STAT2%<>0 THEN PRINT"ERROR":GOTO 580
724 IF STAT3%<>0 THEN PRINT"ERROR":GOTO 580
730 FOR I = 178 TO 255
740 BACGND(I-177)=ASC(MID$(R$,I))
750 NEXT I
760 PRINT R$,R1$,R2$
770 FOR I=1 TO 255
780 BACGND(I+78) = ASC(MID$(R1$,I))
790 NEXT I
800 FOR I = 1 TO 180
810 BACGND(I+333)=ASC(MID$(R2$,I))
820 NEXT I
830 FOR I=1 TO 520 STEP 10
840 FOR J = 1 TO 10
850 PRINT USING "     ###";BACGND(I+J-1);
860 REM LPRINT USING "     ###";bacgnd(I+J-1);
870 NEXT J
880 PRINT
890 REM LIST
900 NEXT I
910 INPUT "DO YOU WANT THE DATA RECORDED? Y/N", ANS$
920 IF ANS$ = 'n' OR ANS$ = "N", THEN GOTO 1080
930 INPUT "INPUT FILE NAME", FILEN$
940 INPUT "input header",A$
950 CLOSE #1
960 OPEN FILEN$ FOR OUTPUT AS #1
```

57

```
970 PRINT #1,A$
980 PRINT #1, MID$(R$,1,80)
990 PRINT #1, MID$(R$,81,80)
1000 PRINT #1, MID$(R$,161,13)
1010 PRINT #1, DATE$,TIME$
1020 FOR I=1 TO 520 STEP 10
1030 FOR J=1 TO 10
1040 PRINT #1, USING "     ###";BACGND(I+J-1);
1050 NEXT J
1060 PRINT #1," "
1070 NEXT I'1075 YMAX=-512
1076 YMIN=512
1080 FOR I=1 TO 520
1090 Y(I)=DTA(I) - BACGND(I)
1091 IF Y(I)<YMIN THEN YMIN=Y(I)
1092 IF Y(I)>YMAX THEN YMAX=Y(i)
1100 NEXT I
1120 FOR I=1 TO 520 STEP 10
1130 FOR J=1 TO 10
1140 PRINT USING "     ####";Y(I+J-1);
1150 NEXT J
1160 PRINT
1170 NEXT I
1180 XMIN=100
1190 XMAX=364
1500 YWMIN=YMIN-.2*(YMAX-YMIN)
1510 YWMAX=YMAX+.15*(YMAX-YMIN)
1520 XWMIN=XMIN-.2*(XMAX-XMIN)
1530 XWMAX=XMAX+.15*(XMAX-XMIN)
1540 SCREEN 2,1
1550 VIEW (0,0)-(639,199)
1560 WINDOW (XWMIN,YWMIN)-(XWMAX,YWMAX)
1580 YLAB$="RELATIVE INTENSITY"
1590 XLAB$="POSITION IN GLITTER PATTERN"
1600 CLS
1620 IXX=PMAP(XMAX,0)
1630 IXM=PMAP(XMIN,0)
1640 IYX=PMAP(YMAX,1)
1650 IYM=PMAP(YMIN,1)
1670 DRAW"BM=IXM;,=IYM;":DRAW"M=IXM;,=IYX;:DRAW"M=IXX;,
     =IYX;"
1680 DRAW"M=IXX;,=IYM;":DRAW"M=IXM;,=IYM;"
1681 LOCATE 23, 25
1682 PRINT XLAB$
1700 FOR X=XMIN TO XMAX
1710 IX=PMAP(x,0)
1720 IY=PMAP(y(X),1)
1730 IF X=XMIN THEN DRAW"BM=IX;,=IY;"
1740 DRAW"M=IX;,=IY;"
1750 NEXT X
1751 LOCATE 6,4:PRINT "RELATIVE"
1790 WIDTH "lpt1:",255
```

58

```
1800 LPRINT CHR$(27)"A"CHR$(7)
2000 V$=INKEY$:IF V$="" THEN 2000
2005 LPRINT CHR$(27)"A"CHR$(12)
2010 SCREEN 0
3000 KEY ON
```

APPENDIX B

LAMBERTIAN REFLECTANCE CALIBRATION

Calibration of the Lambertian reflectance coefficient for the white paper used as a reference in the field was obtained by measuring the ratio of laser radar return signals from a small segment of area, A_t, of the white paper target, to the return signals for specular reflection from a plate glass window.

The Lambertian reflectance, r_L, of the the white paper is given by

$$r_L = \frac{\pi \ r_s \ P_L \ R_L^4}{4 \ A_t \ P_s \ R_s^2}$$

where

r_s = Reflectance of the plate glass window, for two surfaces = .0826 for n = 1.51,

P_L = Laser signal from a small area Lambertian target,

P_s = Laser signal from a plate glass window,

R_L = Distance to the Lambertian target,

R_s = Distance to the plate glass window, and

A_t = Area of the white Lambertian target, small enough to lie within the central flat illumination region of the laser transmitted beam.

The calibration described above was independent of the Lambertian properties of the calibrating target of white paper. That is, it did not matter if the target did not

60

follow the Lambertian behavior of brightness being proportional to the cosine of the angle from the normal. This was because the calibration technique involved only measurements made with the laser radar and hence with a small acceptance angle near normal incidence.

The flatness of the plate glass window used in the calibration was measured by determining the position of the reflected image of an incandescent lamp source. This permitted calculating the radius of curvature. The glass was then treated as a curved mirror, although this correction was very small.

The value of Lambertian reflectance obtained was 0.73 . This is comparable to values of about 0.75 given in many tables of values for the Lambertian reflectance of white paper.

APPENDIX C

TABLE OF DATA

Run #	Glitter Profile Standard Deviations		Effective Laser Reflectance (ρ_{eff})		Inferred Wind Speed
	Upwind (σ_u)	Crosswind (σ_c)	Predicted	Observed	
1	.340	.094	17.4	46.8	13.7
2	.224	.121	20.5	47.6	7.18
3	.175	.141	22.5	42.0	5.60
4	.134	.058	71.4	90.5	2.41
5	.122	.026	175	150	1.72
6	.163	.024	142	182	2.90
7	.081	.030	228	213	1.07
8	.084	.034	194	217	0.92
9	.218	.064	39.8	89.8	5.69
10	.181	.058	52.9	92.7	4.04
11	.241	.120	19.2	73.0	8.45
12	.135	.118	34.8	88.3	4.80
13	.167	.110	30.2	72.3	4.43
14	.150	.100	37.0	86.9	3.58
15	.126	.046	95.8	116	2.39
16	.217	.201	12.7	43.5	10.4
17	.301	.096	19.2	42.3	11.0

62

APPENDIX D

LIGHT SCATTERING CONE

In calculating the expected laser reflectance from a rough water surface, it is necessary to evaluate the size of the cone into which the surface reflects an incident narrow laser beam. However, from geometrical optics, this cone does not have the same included solid angle as the cone measured by observing the glitter pattern obtained with an imager located near a point source illuminator. In the latter case, the light reflects at exactly normal incidence from the facets on the water surface, and the outer limits of the glitter pattern (or sigma points, since a definite outer limit does not strictly exist) occur at a definite angle of inclination of the water surface. However for a vertical pencil beam, the reflected light returns into a cone that has twice the angular spread in both x and y directions, and hence a solid angle that is four times that of the glitter pattern observed at the source with a point source illuminator. This is because the surface which the pencil beam encounters contains facets that are inclined at all the angles which the glitter pattern indicates are in existence, if averaged over a significant period of time. Thus, for example, some of the pencil beam light will encounter surface facets that are

inclined at the angle corresponding to the sigma point of the glitter cone. Because this light is now not at normal incidence to the facet it is encountering, the angle of reflection will be equal to the angle of incidence and the total angle of deviation will be twice the angle of incidence. Since the angle, at the glitter pattern position corresponding to the sigma point, represents the angle of inclination of a facet surface, the angle of deviation from the vertical of the light from a vertically downward pencil beam will be at an angle equal to twice the angle for the glitter pattern sigma point. Since the deflection can be in either the x or y direction, the solid angle of the cone into which the light from the pencil beam is reflected would be expected to have four times the solid angle of the glitter pattern.

Unfortunately, the results obtained with the above interpretation lead to a predicted laser return that is too small by approximately a factor of four, when compared to the observed laser return signal. At this writing, the explanation of this anomaly is not at hand. In order to lead to a reasonable fit to the observed laser return, it has been necessary to assume that the cone into which the reflected light radiates is equal in size to the glitter pattern cone.

LIST OF REFERENCES

1. Gilio, J. P., *Initial Development of a Laser Altimeter*, Master's Thesis, Naval Postgraduate School, September 1985.

2. Petri, K., "Laser Radar Reflectance of Chesapeake Bay Waters as a Function of Wind Speed," *IEEE Transactions on Geoscience Electronics*, V. 15, No. 2, pp 87-96, April 1977.

3. Cox, C. and Munk, W., "Measurement of the Roughness of the Sea Surface from Photographs of the Sun's Glitter," *Journal of the Optical Society of America*, V. 44, pp 838-850, November 1954.

4. Schooley, A., "A Simple Optical Method for Measuring the Statistical Distribution of Water Surface Slopes," *Journal of the Optical Society of America*, V. 44, pp 37-40, January 1954.

5. Swennen, J., "Time-Average Surface-Reflected Energy Received from a Collimated Beam of Radiant Energy Normally Incident on the Ocean Surface," *Journal of the Optical Society of America*, V. 58, pp. 47-51, January 1968.

6. Guinn, J., Plass, G., and Kattawar, G. "Sunlight Glitter on a Wind-Ruffled Sea: Further Studies," *Applied Optics*, V. 18, pp 842-849, 15 March 1959.

7. *468 Digital Storage Oscilloscope*, V. 1, Tektronix, Inc., Beaverton, Oregon, 1981.

INITIAL DISTRIBUTION LIST

		No. Copies
1.	Defense Technical Information Center Cameron Station Alexandria, Virginia 22304-6145	2
2.	Library, Code 0142 Naval Postgraduate School Monterey, California 93943-5002	2
3.	Professor K. E. Woehler, Code 61Wh Chairman, Department of Physics Naval Postgraduate School Monterey, California 93943-5000	2
4.	Professor A. W. Cooper, Code 61Cr Department of Physics Naval Postgraduate School Monterey, California 93943-5000	2
5.	Professor E. C. Crittenden, Jr., Code 61Ct Department of Physics Naval Postgraduate School Monterey, California 93943-5000	2
6	Professor G. W. Rodeback, Code 61Rk Department of Physics Naval Postgraduate School Monterey, California 93943-5000	1
7.	LCDR Carlton M. Bourne Naval Sea Systems Command Headquarters (PMS-405) Washington, D.C. 20362-5101	1
8.	Commander, Naval Sea Systems Command ATTN: CDR M. Mathis, NAVSEA 06W-30 Washington, D.C. 20362-5100	1